



Anisotropic mechanical properties of $Tl_4Ag_{18}Te_{11}$ compound with low thermal conductivity



Aysenur Gencer^a, Ozge Surucu^b, Gokhan Surucu^{c,d,*}, Engin Deligoz^e

^a Karamanoglu Mehmetbey University, Department of Physics, Karaman 70100, Turkey

^b Department of Electrical and Electronics Engineering, Atilim University, Ankara 06836, Turkey

^c Middle East Technical University, Department of Physics, Ankara 06800, Turkey

^d Department of Electric and Energy, Ahi Evran University, Kirsehir 40100, Turkey

^e Aksaray University, Department of Physics, Aksaray 68100, Turkey

ARTICLE INFO

Keywords:

Thermoelectric materials

$Tl_4Ag_{18}Te_{11}$, ab initio

Mechanical properties

Anisotropic elastic properties

ABSTRACT

The anisotropic mechanical properties of $Tl_4Ag_{18}Te_{11}$ compound was investigated elaborately for the first time by using Density Functional Theory calculations with the Vienna Ab-initio Simulation Package in this work. $Tl_4Ag_{18}Te_{11}$ compound was optimized in the I4mm space group and the formation energy was determined as a negative value that is the indication of the experimental synthesizability of this compound. The optimized crystal structure was employed for the calculations of the elastic constants and the obtained values revealed the mechanical stability of $Tl_4Ag_{18}Te_{11}$ compound. The polycrystalline properties were determined such as shear modulus, Poisson's ratio, etc. In addition, the anisotropic elastic properties were presented. The direction dependent sound waves velocities, polarization of the sound waves, enhancement factor and the power flow angle were determined. The thermal conductivity studies were performed and the minimum thermal conductivity ($0.259 \text{ W m}^{-1}\text{K}^{-1}$) and the diffusion thermal conductivity ($0.202 \text{ W m}^{-1}\text{K}^{-1}$) were calculated. This study illustrates the capability of this compound for the thermoelectric materials.

1. Introduction

The world's energy consumption increases with the industrial revolution, population growth, etc. Currently, this energy demand is satisfied mostly from the fossil fuels with the emission of the greenhouse gases that causes global warming. Also, the fossil fuels have limited supply. So, these problems lead to the investigation of the alternative energy sources and energy conversion technologies. The alternative energy sources such as solar and wind energy depending the weather conditions could not satisfy the required energy for the systems all the time [1]. In addition, the heat is dissipated from many systems and this heat releases to the atmosphere. At this stage, the thermoelectric materials get attention due to their capability to use heat to generate electricity [2–4].

Thermoelectric materials are based on the Seebeck effect and the Peltier effect [5,6]. The temperature gradient generates an electrical voltage between two different conductors or semiconductors from hot side to cold side that is the Seebeck effect named after Thomas Johann Seebeck [5,6]. The Peltier effect named after Jean Charles Athanase Peltier, is the opposite of the Seebeck effect and an electrical voltage

drives the heat from one conductor to the other that enables the cooling of one conductor [5,6]. The metals were the first materials investigated for the thermoelectric materials but they have low Seebeck coefficients which is an important parameter for these materials [7]. The functioning of the thermoelectric materials is related to a variable called the thermoelectric figure of merit (ZT) [8–10] defined as $ZT = S^2\sigma T/\kappa$ where S is the Seebeck coefficient, σ is the electrical conductivity and κ is the thermal conductivity. The thermal conductivity is composed of carrier thermal conductivity (κ_e) and lattice thermal conductivity (κ_L). To possess a high ZT value, the material should have a high electrical conductivity while it should have a low thermal conductivity. However, this is contradictory because the electrical conductivity is proportional to thermal conductivity. So, the high ZT material groups have been investigated such as skutterudites [11], Cu based materials [12], chalcogenides [13], zintl phases [14], etc.

Thallium (Tl) based chalcogenides are promising materials for thermoelectric materials having low thermal conductivity [15–18]. $TlScTe_2$ and $TlScSe_2$ were investigated and their thermal conductivities were found to be low with values as $0.43 \text{ W K}^{-1}\text{m}^{-1}$ and $0.66 \text{ W K}^{-1}\text{m}^{-1}$ at

* Corresponding author. Department of Physics, Middle East Technical University, 06800, Ankara, Turkey.

E-mail address: info@gokhansurucu.com (G. Surucu).

room temperature for TiScTe_2 and TiScSe_2 , respectively [17]. Also, AgTlTe and Ag_9TlTe_5 were studied and their room temperature thermal conductivities were measured as $0.25 \text{ W K}^{-1}\text{m}^{-1}$ and $0.22 \text{ W K}^{-1}\text{m}^{-1}$, respectively [19,20]. $\text{Ti}_4\text{Ag}_{18}\text{Te}_{11}$ compound is an n type semiconductor and the experimental study of $\text{Ti}_4\text{Ag}_{18}\text{Te}_{11}$ compound has shown that this compound with $\text{Ti}_{4.05}\text{Ag}_{18}\text{Te}_{11}$ chemical formula has a very low thermal conductivity as $0.19 \text{ W K}^{-1}\text{m}^{-1}$ [21]. Besides, the mechanical and dynamical behavior of materials provide very important information such as stability and stiffness of the materials, micro cracks and plastic deformations etc. which are crucial for the technological applications of the materials. Also, there are limited studies about the elastic properties of some thermoelastic materials such as thallium-tellurium based compounds [22], lead chalcogenides [23], etc. Moreover, there is hardly any study about the anisotropic elastic properties of the experimentally existing $\text{Ti}_4\text{Ag}_{18}\text{Te}_{11}$ thermoelectric material [21]. In the present work, the anisotropic elastic properties of $\text{Ti}_4\text{Ag}_{18}\text{Te}_{11}$ compound have been investigated in detail by using Density Functional Theory (DFT) calculations for the first time.

1.1. Computational details

The theoretical investigation of $\text{Ti}_4\text{Ag}_{18}\text{Te}_{11}$ compound has been executed using VASP (Vienna Ab-initio Simulation Package) [24,25] on the basis of the Density Functional Theory. The calculations have been performed with the Perdew-Burke-Ernzerhof (PBE) functional of the Generalized Gradient Approximation (GGA) [26] for the exchange correlation of the electron-electron interaction. The Projector Augmented Wave (PAW) method [27,28] has been employed for the electron-ion interactions. The cut off energy for the planewaves is taken as 480 eV and a gamma centered grid [29] has been used to obtain k-points as $2 \times 2 \times 1$ k-points. The calculations have been converged up to 10^{-7} eV energy convergence and 10^{-8} eV/Å force convergence criteria. The valence electron configurations of Tl, Ag and Te atoms has been taken as $6s^26p^1$, $4d^{10}5s^1$ and $5s^25p^4$, respectively. The X-ray diffraction pattern of $\text{Ti}_4\text{Ag}_{18}\text{Te}_{11}$ compound has been obtained using VESTA software [30] with Cu K α source that have 1.541 Å wavelength. The mechanical properties have been studied using stress-strain method [24,25,31]. These constants have been employed to ELATE software [32] in order to

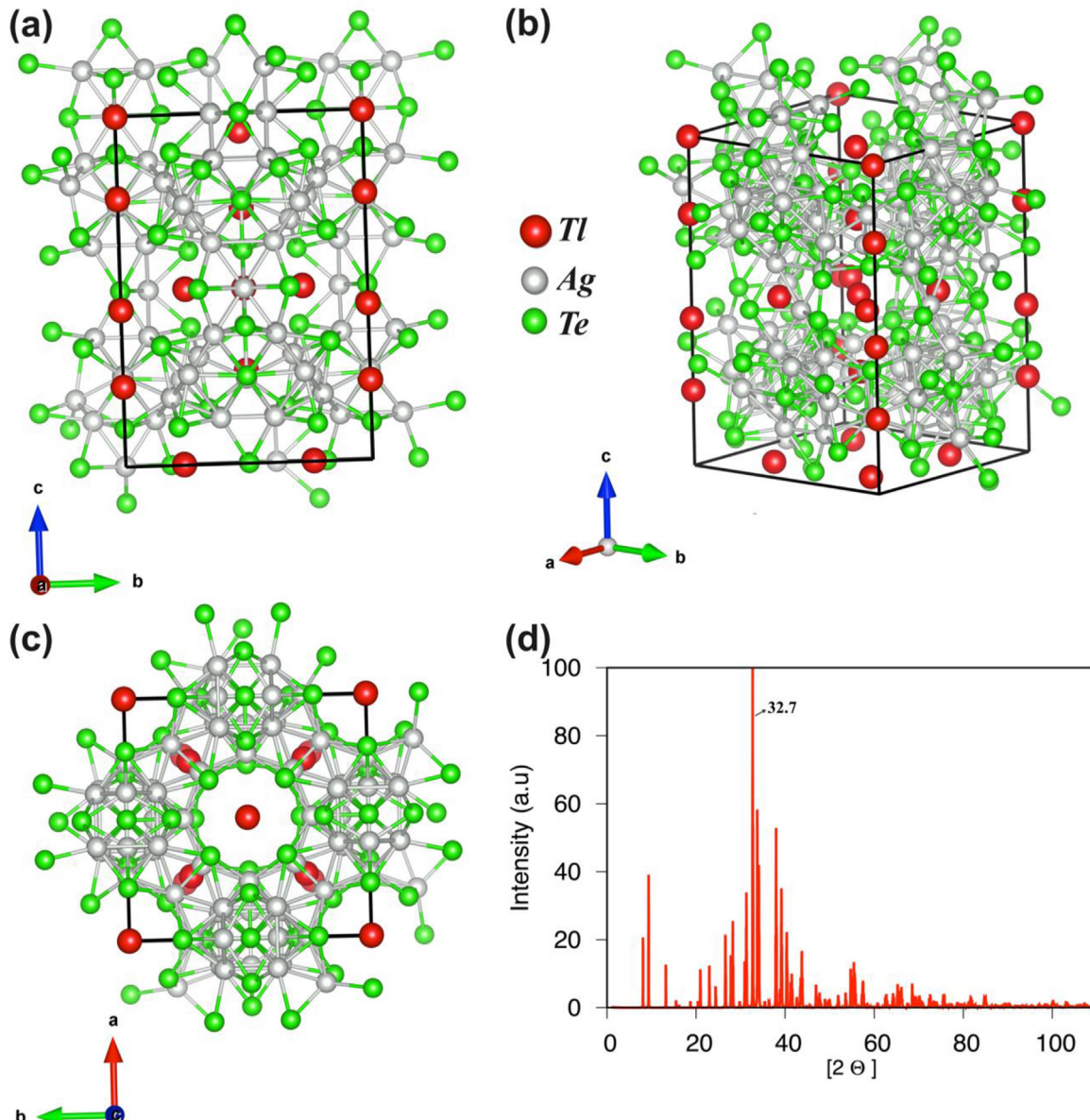


Fig. 1. (a, b, c) The unit cell in different direction and (d) X-ray diffraction pattern for $\text{Ti}_4\text{Ag}_{18}\text{Te}_{11}$ compound.

obtain the anisotropic elastic properties. Also, the direction dependent sound wave velocities have been obtained using Christoffel software [33] - a python tool that solves the Christoffel equation [34] using the elastic stiffness matrix.

2. Results and discussions

$\text{Tl}_4\text{Ag}_{18}\text{Te}_{11}$ compound has a tetragonal crystal structure with I4mm space group as shown in Fig. 1 with the primitive cell and the unit cell. This crystal structure has been optimized and the obtained lattice constants and the formation energy determined using equation given in Refs. [35] are listed in Table 1. The determined negative value for the formation energy is an indication of the experimental synthesizability that is consistent with Ref [21]. The calculated lattice parameters and the formation energy are consistent with Ref [36,37]. In addition, the X-ray diffraction pattern for $\text{Tl}_4\text{Ag}_{18}\text{Te}_{11}$ compound has been shown in Fig. 1d that could be useful for future experimental studies and the maximum scattering angle (2θ) is 32.7° for (0 4 4) direction.

The mechanical stability and the anisotropic elastic properties are very crucial for various industrial applications. The optimized crystal structure has been used to determine the elastic constants (C_{ij}) that are essential to understand the mechanical properties. The elastic constants of $\text{Tl}_4\text{Ag}_{18}\text{Te}_{11}$ compound have six independent components because of the symmetry properties of the I4mm space group, namely C_{11} , C_{12} , C_{13} , C_{33} , C_{44} , and C_{66} in Young notation. In order to understand the flexibility and mechanical stability of $\text{Tl}_4\text{Ag}_{18}\text{Te}_{11}$ compound, the elastic constants (C_{ij}) for a tetragonal crystal, have been calculated using the stress-strain approach [24], as seen in Table 2.

The Born stability criteria [38,39] must be satisfied for this compound in order to be a mechanically stable compound. The Born stability criteria for a tetragonal crystal structure is given as;

$$\begin{aligned} C_{11} > 0, \quad C_{33} > 0, \quad C_{44} > 0, \quad C_{66} > 0 \\ (C_{11}-C_{12}) > 0, \quad (C_{11}+C_{33}-2C_{13}) > 0 \\ [2(C_{11}+C_{12})+C_{33}+4C_{13}] > 0 \end{aligned} \quad (1)$$

As can be deduced from the Table, the stability criteria have been satisfied for $\text{Tl}_4\text{Ag}_{18}\text{Te}_{11}$ compound. Hence, it is concluded that $\text{Tl}_4\text{Ag}_{18}\text{Te}_{11}$ compound is a mechanically stable.

In addition, the polycrystalline properties such as bulk modulus, shear modulus, Poisson's ratio, etc. as listed in Table 2 could be determined using these constants. The bulk modulus (B) is the resistance to shape deformations against a hydrostatic pressure. The shear modulus (G) is the resistance to shear stress. The Young's modulus (E) is the resistance to uniaxial stress. It can be noted that the calculated Young's and shear moduli are small, showing that $\text{Tl}_4\text{Ag}_{18}\text{Te}_{11}$ should have low thermal conductivity. Poisson's ratio can be used to determine the bonding nature of the solids. If a solid is covalent bound the ν value is 0.1, for metallic solids the ν value is 0.33. Also, the approach of the ν value around 0.5 improves the plasticity [35]. Table 2 reveals that $\text{Tl}_4\text{Ag}_{18}\text{Te}_{11}$ compound has metallic bonding. Similar to the Poisson's ratio, the G/B ratio could also be used for the determination of the bonding characteristics. The G/B ratios around 1.1, 0.8 and 0.3 indicate the dominantly covalent bonding, ionic bonding and metallic bonding, respectively [35]. As can be concluded from Table 2, the calculated G/B ratio for $\text{Tl}_4\text{Ag}_{18}\text{Te}_{11}$ compound indicates the metallic bonding and it is the consistent with the Poisson's ratio. The ductile or the brittle nature of a compound could be determined with the B/G ratio and the values for the

B/G ratio lower than 1.75 implies the brittleness while higher than 1.75 indicates the ductility [35]. $\text{Tl}_4\text{Ag}_{18}\text{Te}_{11}$ compound is a ductile material with the B/G ratio higher than 1.75.

The shear anisotropic factors (A_1 , A_2 , A_3) have been calculated using the following equations given in Ref. [40] in which these equations are mentioned as the most useful ones to provide in-plane phonon-focusing information for tetragonal crystals. The shear anisotropic factors in different planes of a crystal give the degree of elastic anisotropy of a material.

$$\begin{aligned} A_1 &= \frac{C_{44}(C_{11} + 2C_{13} + C_{33})}{(C_{11}C_{33} - C_{13}^2)} \quad \text{for } (100) \text{ or } (010) \\ A_2 &= \frac{C_{44}(C_L + 2C_{13} + C_{33})}{(C_L C_{33} - C_{13}^2)} \quad \text{for } (1\bar{1}0) \\ A_3 &= \frac{2C_{66}}{(C_{11} - C_{12})} \quad \text{for } (001) \end{aligned} \quad (2)$$

here $C_L = C_{66} + \frac{(C_{11} + C_{12})}{2}$ is the constant. The shear anisotropic factors are calculated as 0.69 for A_1 , 0.64 for A_2 and 1.44 for A_3 . The deviation from the unity indicates the anisotropy for a crystal. Hence, it can be deduced that there is an anisotropy for $\text{Tl}_4\text{Ag}_{18}\text{Te}_{11}$ crystal both in (100), (010), (110) and (001) planes. Moreover, the universal anisotropy index (A^U) and percent elastic anisotropy in shear and compression (A_G , A_B) are calculated by the following common relation given in Refs. [40,41].

$$\begin{aligned} A^U &= 5 \frac{G_V}{G_R} + \frac{B_V}{B_R} - 6 \\ A_G &= \frac{|G_V - G_R|}{|G_V + G_R|} \cdot 100 \\ A_B &= \frac{|B_V - B_R|}{|B_V + B_R|} \cdot 100 \end{aligned} \quad (3)$$

where B and G are the bulk and shear modulus, and the subscripts V and R represent the Voigt and Reuss approximation. The shear anisotropic factors are calculated as 0.69 for A_1 , 0.64 for A_2 and 1.44 for A_3 . The universal anisotropy index and percent elastic anisotropy in shear and compression are calculated as 0.215 for A^U , 2.103 for A_G and 0.003 for A_B . For isotropic materials, the universal index and percent anisotropy in shear and compression are taken as zero. A value of zero ($B_R=B_V$) is associated with elastic isotropy, while a value of 100% is associated with the largest anisotropy [40].

The anisotropic elastic properties of materials are crucial that provides the information for microcracks, plastic deformations, etc [41]. This information is essential for the technological applications of the materials. $\text{Tl}_4\text{Ag}_{18}\text{Te}_{11}$ compound has been considered for the elastic anisotropy and Young's modulus, linear compressibility, shear modulus and Poisson's ratio have been studied for the direction dependent properties in three dimensions (3D) and two dimensions (2D) as shown in Fig. 2. The spherical or the circular shapes indicate the elastic isotropy while the distorted shapes indicate the elastic anisotropy. Also, the green shapes or curves show the minimum values for the parameter and the blue ones show the maximum values. As can be seen from Fig. 2, the only isotropic parameter is the linear compressibility that has about spherical shapes in all planes. It is noticed that C_{33} is larger than C_{11} , indicating that the x-axis is more compressible than the z-axis for compound. Also,

Table 1

The determined lattice constants (a and c) and the formation energy (ΔE_F in eV/atom) for $\text{Tl}_4\text{Ag}_{18}\text{Te}_{11}$ compound.

Compound	Reference	a (Å)	b (Å)	c (Å)	α	β	γ	ΔE_F
$\text{Tl}_4\text{Ag}_{18}\text{Te}_{11}$	Primitive Cell	13.374	13.374	13.371	60.043	60.043	59.914	-0.155
	Unit Cell	13.353	13.353	18.943	90	90	90	
	Primitive Cell [36]	13.408	13.408	13.385	60.056	60.056	59.976	-0.135
	Unit Cell [36]	13.394	13.394	18.981	90	90	90	

Table 2

The elastic constants (C_{ij} in GPa) and mechanical properties as bulk modulus (B in GPa), shear modulus (G in GPa), Young's modulus (E in GPa), Poisson's ratio (ν), G/B ratio and B/G ratio for $Tl_4Ag_{18}Te_{11}$ compound.

Compound	C_{11}	C_{12}	C_{13}	C_{33}	C_{44}	C_{66}	B	G	E	ν	G/B	B/G
$Tl_4Ag_{18}Te_{11}$	75.6	43.5	35.6	82.0	15.0	23.1	51.4	19.7	52.5	0.33	0.383	2.609

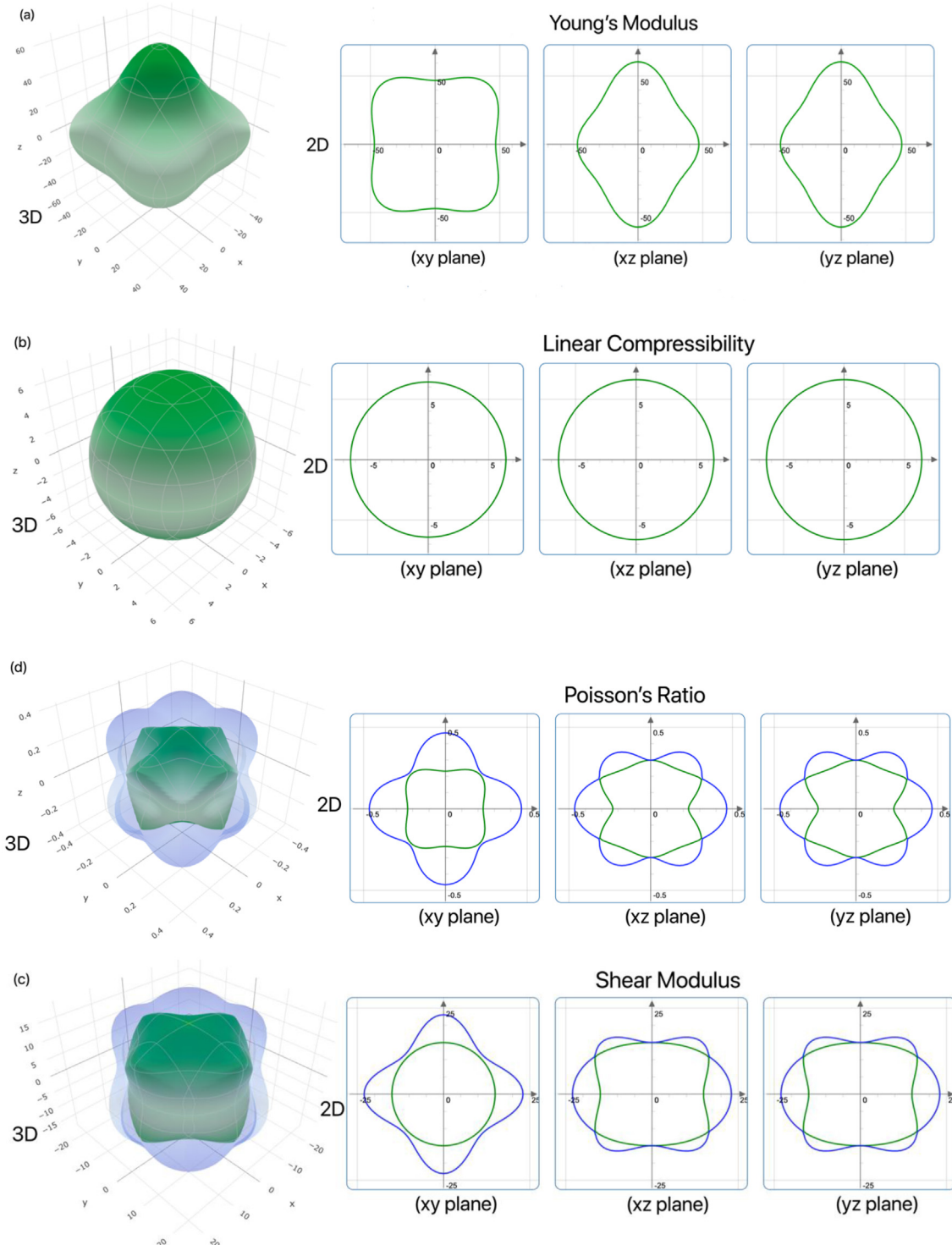


Fig. 2. The direction dependent (a) Young's modulus, (b) linear compressibility, (c) shear modulus and (d) Poisson's ratio of $Tl_4Ag_{18}Te_{11}$ compound.

C_{44} is lower than C_{66} , indicating that shear along the (001) plane is easier than shear along the (100) plane.

The Young's modulus is anisotropic in all planes and the maximum values have been obtained in x plane, z plane and 45° of xy plane with 60.7 GPa value. The shear modulus is also anisotropic in all planes and similar behavior in xz and yz planes have been obtained with 23.4 GPa maximum values. The Poisson's ratio is also anisotropic in all planes and similar to the shear modulus, the similar behavior in xz and yz planes have been obtained with 0.5 maximum value.

The sound wave velocities could be determined using the elastic constants. For $Tl_4Ag_{18}Te_{11}$ compound, the direction dependent sound wave velocities have been determined using the Christoffel tool [33]. In experiments, the sound wave velocities are measured and the elastic constants could be determined using these velocities. Here, the approach is inverse. The elastic constants are determined and then the Christoffel tool uses these determined values to obtain the sound wave velocities. There are three sound wave velocities where one is the longitudinal sound wave velocity (V_{LA}) and the others are the transverse sound wave velocities (V_{TA}) in two perpendicular directions. The relation between the sound wave velocities in and the elastic constants are as follows [42]:

$$\begin{aligned} V_{LA}[100] &= (C_{11}/\rho)^{1/2} \\ V_{LA}[001] &= (C_{33}/\rho)^{1/2} \\ V_{TA}[110]_{<001>} &= (C_{44}/\rho)^{1/2} \\ V_{TA}[110]_{<100>} &= (C_{66}/\rho)^{1/2} \end{aligned} \quad (4)$$

where, ρ is the density of $Tl_4Ag_{18}Te_{11}$ compound. From Equation (4), one can conclude that the longitudinal wave velocity along [001] direction is higher than the longitudinal wave velocity along [100] direction due to C_{33} is higher than C_{11} . For the transverse wave velocity, it is higher along [110]_{<100>} direction than [110]_{<001>} direction because C_{66} is higher than C_{44} .

Fig. 3 is plotted due to the results obtained by using Equation (4) and it shows the group wave velocity, the phase wave velocity, the polarization of the sound waves, the enhancement factor and the power flow angle for $Tl_4Ag_{18}Te_{11}$ compound in three dimensions. The group wave velocity, which is the superposition of the phase wave velocities, is shown in Fig. 3a. As seen from the figure, the primary mode is found to be the fastest along z direction (001). For the secondary mode for the group wave velocity, the fast-secondary mode has high values in x and y directions and low values in z direction and in between x, y and z direction. In contrast to the fast secondary for the group wave velocity, the slow secondary is slow along x, y and z directions and it is fast in between x, y and z directions. The phase wave velocity has similar behavior with the group wave velocity as can be seen from Fig. 3b. The polarization of the sound waves is shown in Fig. 3c and the primary mode has pseudo-transverse polarization in z direction while it has pseudo-longitudinal polarization in x and y directions. In contrast to the primary mode, the fast-secondary mode has pseudo-longitudinal polarization in z direction while it has pseudo-transverse polarization in x and y directions. The slow secondary mode has pseudo-longitudinal polarization in all axis. The enhancement factor, which is the ratio of the direction of the group wave velocity to the direction of the phase wave, is shown in Fig. 3d. The enhancement factor has low values along x, y and z directions for the slow secondary while it has high values x and y directions for the fast secondary. The primary mode for the enhancement factor has low values along x and y directions and high values along z direction and in between x and y directions. Moreover, Fig. 3e shows the power flow ang which is the angle between the group wave velocity and the phase wave velocity. The power flow angle varies for the primary mode, the fast-secondary mode and the slow secondary mode due to the difference for the group and phase wave velocities for these modes. As a result, it is deduced that the primary modes in group wave velocity, phase wave velocity, polarization of sound waves, enhancement factor and power flow angle for $Tl_4Ag_{18}Te_{11}$ compound have the highest values along the z direction (001). By considering Fig. 1c, Tl atoms are located inside large channels

of perfectly ordered Te and Ag atoms which are at the vertices of squares perpendicular to the (001) direction. This arrangement of large channel connected by smaller channels is reproduced along the three equivalent directions (100), (010) and (001). Hence, having the highest values in primary modes along the z-direction (001) is and expected result.

The thermal conductivity (λ) of $Tl_4Ag_{18}Te_{11}$ compound has been studied that is a major parameter for the thermoelectric applications. Cahill [43], Clarke [44] and Long [45] models are used to calculate the values of minimum thermal conductivity and Synder [46] model is used to calculate the diffusion thermal conductivity given in Equations (5)–(8);

$$\lambda_{min(Cahill)} = \frac{k_B}{2.48} n^{2/3} (V_L + 2V_T) \quad (5)$$

$$\lambda_{min(Clark)} = 0.87 k_B M_a^{-3/2} E^{2/3} \rho^{1/6} \quad (6)$$

$$\lambda_{min(Long)} = \left\{ \frac{1}{3} \left[2(2+2\nu)^{3/2} + \left(\frac{1}{1-\nu} - \nu \right)^{3/2} \right] \right\}^{-1/3} k_B n^{2/3} \left(\frac{E}{\rho} \right)^{1/2} \quad (7)$$

$$\lambda_{diff} = 0.76 n^{2/3} k_B V_m \quad (8)$$

where, ρ (= 8.184 g.cm⁻³) is the density, k_B is the Boltzman constant, n is the density of number of the atoms per volume, M_a is the average mass per atom, V_L is the average longitudinal sound wave velocity, V_T is the average transverse sound wave velocity and V_m is the average wave velocity. For $Tl_4Ag_{18}Te_{11}$ compound, the number of atoms per volume (n) has been determined as 3.9×10^{28} m⁻³. In addition, the average longitudinal sound wave velocity (V_L), the average transverse sound wave velocity (V_T) and the average wave velocity (V_m) have been calculated by using the relations given in Refs. [40] as 3039 m/s, 1489 m/s and 1672 m/s, respectively. The calculated minimum thermal conductivity (λ) values along with the measured values for $Tl_{4.05}Ag_{18}Te_{11}$ compound in Ref. [21] are given in Table 3.

As can be concluded from the table that the minimum thermal conductivity using Long model in the present study is very close to the obtained result using Cahill model in Ref. [21]. And there is a discrepancy in between the calculated and the measured diffusion thermal conductivity values. On the other hand, the measured thermal conductivity for pristine $Tl_4Ag_{18}Te_{11}$ compound ranges from 0.44 W m⁻¹K⁻¹ at 320 K to 0.35 W m⁻¹K⁻¹ at 500 K [21]. The differences in the results could be consisted of the measurement uncertainties which is also stated in the study given in Ref. [21]. The calcultated thermal conductivities are small, showing that $Tl_4Ag_{18}Te_{11}$ has promising thermal-insulating application in engineering.

2.1. Conclusion

$Tl_4Ag_{18}Te_{11}$ compound has been studied for the mechanical and anisotropic elastic properties by using the Vienna Ab-initio Simulation Package based on Density Functional Theory (DFT). The calculated negative formation energy of $Tl_4Ag_{18}Te_{11}$ compound is the indication of the experimental synthesizability of this compound. In addition, the elastic constants satisfy the Born stability criteria that shows the mechanical stability as well. The values of the Poisson's ratio and the G/B ratio shows that $Tl_4Ag_{18}Te_{11}$ compound has dominantly metallic bonding. In addition, $Tl_4Ag_{18}Te_{11}$ compound is a ductile material. The anisotropic elastic properties show that $Tl_4Ag_{18}Te_{11}$ compound is an anisotropic material with values as 0.69 for A_1 in (100) or (010) planes, 0.64 for A_2 in (110) plane and 1.44 for A_3 in (001) plane. The direction dependent sound wave velocities show that the longitudinal wave velocity along [001] direction is higher than the longitudinal wave velocity along [100] direction and the transverse wave velocity is higher along [110]_{<100>} direction than [110]_{<001>} direction. Also, the primary mode has pseudo-transverse polarization in z direction while it has pseudo-

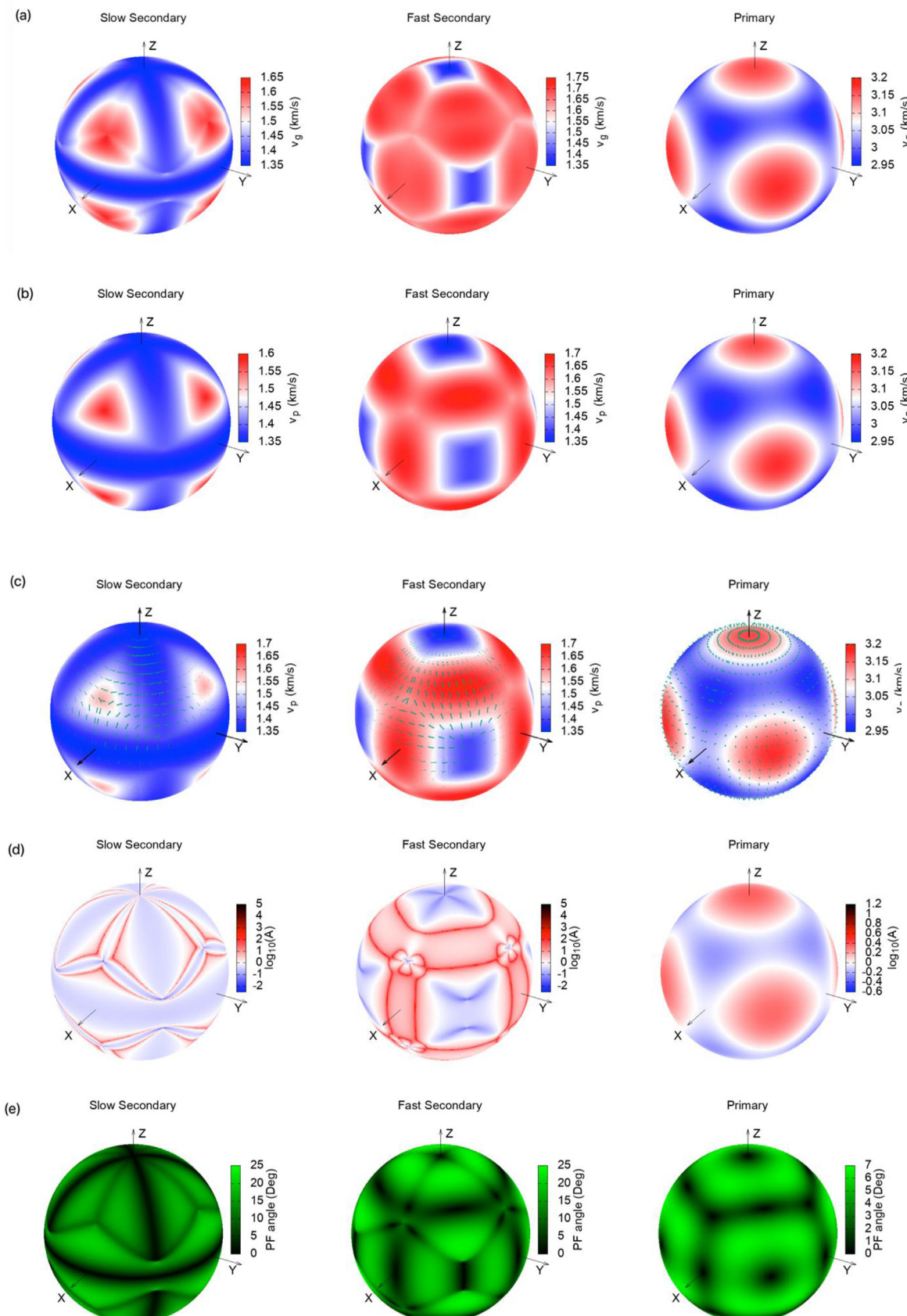


Fig. 3. (a) Group wave velocity, (b) phase wave velocity, (c) polarization of sound waves, (d) enhancement factor and (e) power flow angle for $Tl_4Ag_{18}Te_{11}$ compound.

Table 3

The minimum thermal conductivities (λ_{min} in $W.m^{-1}.K^{-1}$) and diffusion thermal conductivity (λ_{diff} in $W.m^{-1}.K^{-1}$) for $Tl_4Ag_{18}Te_{11}$ compound.

Compound	λ_{min}			λ_{diff}
	Cahill model	Clarke model	Long model	
$Tl_4Ag_{18}Te_{11}$ (This work)	0.386	0.337	0.259	0.202
$Tl_4.05Ag_{18}Te_{11}$ (Experimental [21])	0.270	0.210		0.170

longitudinal polarization in x and y directions. Moreover, the minimum and diffusion thermal conductivities have been determined that are consistent with the experimental results. This study revealing the mechanical and anisotropic elastic properties of $Tl_4Ag_{18}Te_{11}$ compound could lead future investigations especially for the thermoelectric applications due to its lower thermal conductivity.

Declaration of competing interest

The authors declare that they have no known competing financial interests or personal relationships that could have appeared to influence the work reported in this paper.

CRediT authorship contribution statement

Aysenur Gencer: Investigation, Writing - original draft, Data curation. **Ozge Surucu:** Investigation, Writing - original draft. **Gokhan Surucu:** Conceptualization, Methodology, Software, Writing - review & editing. **Engin Deligoz:** Supervision, Writing - review & editing.

References

- [1] A.M.A. Acuzar, I.P.E. Arguelles, J.C.S. Elisan, J.K.D. Gobenciong, A.M. Soriano, J.M.B. Rocamora, Effects of weather and climate on renewable energy resources in a distributed generation system simulated in Visayas, Philippines, in: 2017IEEE 9th International Conference on Humanoid, Nanotechnology, Information Technology, Communication and Control, Environment and Management (HNICEM), 2017, pp. 1–6.
- [2] L. Yang, Z.-G. Chen, M.S. Dargusch, J. Zou, High performance thermoelectric materials: progress and their applications, *Adv. Energy Mater.* 8 (6) (Feb. 2018) 1701797.
- [3] G.J. Snyder, E.S. Toberer, Complex thermoelectric materials, *Nat. Mater.* 7 (2) (Feb. 2008) 105–114.
- [4] S. Twaha, J. Zhu, Y. Yan, B. Li, A comprehensive review of thermoelectric technology: materials, applications, modelling and performance improvement, *Renew. Sustain. Energy Rev.* 65 (Nov. 2016) 698–726.
- [5] J.F. Li, W.S. Liu, L.D. Zhao, M. Zhou, High-performance nanostructured thermoelectric materials, *NPG Asia Mater.* 2 (4) (Oct. 2010) 152–158.
- [6] X. Zhang, L.D. Zhao, Thermoelectric materials: energy conversion between heat and electricity, *J. Mater.* 1 (2) (Jun. 2015) 92–105.
- [7] B. Cai, H. Hu, H.-L. Zhuang, J.F. Li, Promising materials for thermoelectric applications, *J. Alloys Compd.* 806 (Oct. 2019) 471–486.
- [8] J. He, T.M. Tritt, Advances in thermoelectric materials research: looking back and moving forward, *Science* 357 (Sep. 2017) 6358.
- [9] Y. Shi, C. Sturm, H. Kleinke, Chalcogenides as thermoelectric materials, *J. Solid State Chem.* 270 (Feb. 2019) 273–279.
- [10] G.J. Snyder, E.S. Toberer, Complex thermoelectric materials, *Nat. Mater.* 7 (2) (Feb. 2008) 105–114.
- [11] G. Rogl, P. Rogl, Skutterudites, a most promising group of thermoelectric materials, *Curr. Opin. Green Sustain. Chem.* 4 (Apr. 2017) 50–57.
- [12] P. Qiu, X. Shi, L. Chen, Cu-based thermoelectric materials, *Energy Storage Mater.* 3 (Apr. 2016) 85–97.
- [13] I. Nandhakumar, N.M. White, S. Beeby (Eds.), *Thermoelectric Materials and Devices*, Royal Society of Chemistry, Cambridge, 2016.
- [14] E.S. Toberer, A.F. May, G.J. Snyder, Zintl chemistry for designing high efficiency thermoelectric materials, *Chem. Mater.* 22 (3) (Feb. 2010) 624–634.
- [15] B. Wölfig, C. Kloc, J. Teubner, E. Bucher, High performance thermoelectric Tl_9BiTe_6 with an extremely low thermal conductivity, *Phys. Rev. Lett.* 86 (19) (May 2001) 4350–4353.
- [16] Michael A. McGuire, Thomas K. Reynolds, Francis J. DiSalvo, Exploring Thallium Compounds as Thermoelectric Materials: Seventeen New Thallium Chalcogenides, 2005.
- [17] V.S. Aswathy, C.R. Sankar, M.R. Varma, A. Assoud, M. Bieringer, H. Kleinke, Thermoelectric properties and thermal stability of layered chalcogenides, $TlScQ_2$, $Q = Se, Te$, *Dalt. Trans.* 46 (48) (Dec. 2017) 17053–17060.
- [18] C. Uher, *Materials Aspect of Thermoelectricity*, first ed., CRC Press, Boca Raton, 2017 <https://doi.org/10.1201/9781315197029>.
- [19] K. Kuroaki, H. Uneda, H. Muta, S. Yamanaka, Extremely low thermal conductivity of $AgTlTe$, *J. Alloys Compd.* 395 (1–2) (May 2005) 304–306.
- [20] K. Kuroaki, A. Kosuga, H. Muta, M. Uno, S. Yamanaka, Ag_9TlTe_5 : A high-performance thermoelectric bulk material with extremely low thermal conductivity, *Appl. Phys. Lett.* 87 (6) (Aug. 2005), 061919.
- [21] Y. Shi, et al., Ultralow thermal conductivity of $Tl_4Ag_{18}Te_{11}$, *J. Mater. Chem. C* 7 (26) (Jul. 2019) 8029–8036.
- [22] X. Tao, P. Jund, R. Viennois, J.-C. Tedenac, Physical properties of thallium–tellurium based thermoelectric compounds using first-principles simulations, *J. Phys. Chem.* 115 (31) (Aug. 2011) 8761–8766.
- [23] G. Li, et al., Micro- and macromechanical properties of thermoelectric lead chalcogenides, *ACS Appl. Mater. Interfaces* 9 (46) (Nov. 2017) 40488–40496.
- [24] G. Kresse, J. Furthmüller, Efficient iterative schemes for *ab initio* total-energy calculations using a plane-wave basis set, *Phys. Rev. B* 54 (16) (Oct. 1996) 11169–11186.
- [25] G. Kresse, J. Furthmüller, Efficiency of ab-initio total energy calculations for metals and semiconductors using a plane-wave basis set, *Comput. Mater. Sci.* 6 (1) (Jul. 1996) 15–50.
- [26] J.P. Perdew, K. Burke, M. Ernzerhof, Generalized gradient approximation made simple, *Phys. Rev. Lett.* 77 (18) (Oct. 1996) 3865–3868.
- [27] P.E. Blöchl, Projector augmented-wave method, *Phys. Rev. B* 50 (24) (Dec. 1994) 17953–17979.
- [28] G. Kresse, D. Joubert, From ultrasoft pseudopotentials to the projector augmented-wave method, *Phys. Rev. B* 59 (3) (Jan. 1999) 1758–1775.
- [29] J.D. Pack, H.J. Monkhorst, Special points for Brillouin-zone integrations—a reply, *Phys. Rev. B* 16 (4) (Aug. 1977) 1748–1749.
- [30] K. Momma, F. Izumi, VESTA3 for three-dimensional visualization of crystal, volumetric and morphology data, *J. Appl. Crystallogr.* 44 (6) (Dec. 2011) 1272–1276.
- [31] Y. Le Page, P. Saxe, Symmetry-general least-squares extraction of elastic data for strained materials from *ab initio* calculations of stress, *Phys. Rev. B* 65 (10) (Feb. 2002) 104104.
- [32] R. Gaillac, P. Pullumbi, F.X. Coudert, ELATE: an open-source online application for analysis and visualization of elastic tensors, *J. Phys. Condens. Matter* 28 (27) (Jul. 2016) 275201.
- [33] J.W. Jaeken, S. Cottenier, Solving the Christoffel equation: phase and group velocities, *Comput. Phys. Commun.* 207 (Oct. 2016) 445–451.
- [34] F.I. Fedorov, General equations of the theory of elasticity, in: *Theory of Elastic Waves in Crystals*, Springer US, Boston, MA, 1968, pp. 1–33.
- [35] M.B. Baysal, G. Surucu, E. Deligoz, H. Ozisik, The effect of hydrogen on the electronic, mechanical and phonon properties of $LaMgNi_4$ and its hydrides for hydrogen storage applications”, *Int. J. Hydrogen Energy* 43 (2018) 23397–23408.
- [36] K. Persson, Materials Data on $Tl_4Ag_{18}Te_{11}$ (SG:107) by Materials Project, 2016, <https://doi.org/10.17188/1263363>. United States: N. p.
- [37] A. Jain, S.P. Ong, G. Hautier, W. Chen, W.D. Richards, S. Dacek, S. Cholia, D. Gunter, D. Skinner, G. Ceder, K.A. Persson, The Materials Project: a materials genome approach to accelerating materials innovation, *Apl. Mater.* 1 (2013), 011002.
- [38] Z. Wu, E. Zhao, H. Xiang, X. Hao, X. Liu, J. Meng, Crystal structures and elastic properties of superhard IrN_2 and IrN_3 from first principles, *Phys. Rev. B* 76 (5) (Aug. 2007), 054115.
- [39] M. Born, On the stability of crystal lattices. I, *Math. Proc. Camb. Phil. Soc.* 36 (2) (Apr. 1940) 160–172.
- [40] A. Erkisi, G. Surucu, E. Deligoz, The structural, electronic, magnetic, and mechanical properties of perovskite oxides $PbM_{1/2}Nb_{1/2}O_3$ ($M = Fe, Co$ and Ni), *Int. J. Mod. Phys. B* 32 (2018) 1850057–1850077.
- [41] G. Surucu, Investigation of structural, electronic, anisotropic elastic, and lattice dynamical properties of MAX phases borides: an Ab-initio study on hypothetical M_2AB ($M = Ti, Zr, Hf$; $A = Al, Ga, In$) compounds, *Mater. Chem. Phys.* 203 (Jan. 2018) 106–117.
- [42] G. Surucu, K. Colakoglu, E. Deligoz, N. Korozlu, First-Principles study on the MAX phases $Ti_{n+1}GaN_n$ ($n = 1, 2$, and 3), *J. Electron. Mater.* 45 (8) (Aug. 2016) 4256–4264.
- [43] D.G. Cahill, S.K. Watson, R.O. Pohl, Lower limit to the thermal conductivity of disordered crystals, *Phys. Rev. B* 46 (1992) 6131–6140.
- [44] D.R. Clarke, C.G. Levi, Materials design for the next generation thermal barrier coatings, *Annu. Rev. Mater. Res.* 33 (2003) 383–417.
- [45] J. Long, C. Shu, L. Yang, M. Yang, Predicting crystal structures and physical properties of novel superhard p-BN under pressure via first-principles investigation, *J. Alloys Compd.* 644 (Sep. 2015) 638–644.
- [46] M.T. Agne, R. Hanus, G.J. Snyder, Minimum thermal conductivity in the context of diffusion-mediated thermal transport, *Energy Environ. Sci.* 11 (3) (Mar. 2018) 609–616.